



Performance Enhancement of GPS/INS Integrated Navigation System Using Wavelet Based De-Noising Method

N. Davari^{1,*}, A. Gholami², M. Shabani³

1- Ph.D. Student, Department of Electrical and Computer Engineering, Isfahan University of Technology, Isfahan, 84156-83111, Iran

2- Associate Professor, Department of Electrical and Computer Engineering, Isfahan University of Technology, Isfahan, 84156-83111, Iran

3- M.Sc., Department of Electrical and Computer Engineering, Isfahan University of Technology, Isfahan, 84156-83111, Iran

(Received 3 July 2015, Accepted 31 July 2016)

ABSTRACT

The accuracy of Inertial Navigation System (INS) is limited mainly by inertial sensors imperfections. Before using inertial signals in the datafusion algorithm, noise removal procedure should be done. In order to remove the noise, wavelet decomposition method is used in which the raw data are decomposed into high and low-frequency data sets. In this study, wavelet multi-level of decomposition technique is used as an efficient pre-filter method for inertial measurements to improve the performance of INS. This technique improves navigation accuracy by eliminating the high-frequency noise of inertial measurements. Optimum values of the level of decomposition are selected to obtain minimum error. Successfully performing the de-noising process improves the sensors' signal-to-noise ratios and removes short term errors mixed with motion dynamics and finally provides cleaner and more reliable data to the INS. In this paper, the performance of an error state Kalman filter based GPS/INS integrated navigation system is studied using real measurement during GPS outages. The GPS/INS integrated navigation system used in this work is the loosely coupled structure. Results show that the average value of the root mean square of the position errors (as a measure of the quality of de-noising) during GPS outages using the WMRA procedure is reduced about 14% compared to those using the raw inertial measurements.

KEYWORDS:

GPS/INS Integrated Navigation, GPS Outages, Wavelet Analysis, Error State Kalman Filter, Level of Decomposition

Please cite this article using:

Davari, N., Gholami, A., and Shabani, M., 2016. "Performance Enhancement of GPS/INS Integrated Navigation System Using Wavelet Based De-Noising Method". *Amirkabir International Journal of Electrical and Electronics Engineering*, 48(2), pp. 101–111.

DOI: 10.22060/ej.2016.824

URL: http://eej.aut.ac.ir/article_821.html

*Corresponding Author, Email: n.davari@ec.iut.ac.ir



1- Introduction

Most navigation systems use inertial sensors (accelerometers and gyroscopes). An inertial navigation system (INS) has a good accuracy in a short time, but the error grows with the elapse of time without bounds, while GPS has a high accuracy in a long time. Thus, INS and GPS integration could improve navigation accuracy for all times [1]. Conventional Kalman filtering (KF) [2] has been the widely the implemented and accepted procedure for integrating the inertial navigation systems (INS) with auxiliary sensors. The Kalman filter has been implemented in two approaches, total state space and error state space methods, which are named direct and indirect filtering, respectively [3,4]. In recent years, the indirect filtering is used mostly in the integrated navigation systems [5,6]. Some literature reported the direct filtering based integrated navigation system [7-9]. In the case of GPS outages (signal blockages), the INS positioning error will increase in time until the GPS signals are available again. As soon as the GPS signals become available, it provides position information that may lead to compensation of INS errors [10].

The primary concern when working with a low-performance inertial measurement unit (IMU) is that the navigation solution degrades rapidly in the absence of an aiding source (which is mainly GPS). However, the navigation is still facing problem in places where the GPS signal gets lost, that commonly occur in urban areas and in unsuitable weather condition. In the case of GPS outages, the INS is used alone for positioning until the GPS signals are available again. One of the major issues that limits the INS accuracy, as a stand-alone navigation system, is the level of sensor imperfections especially its noise [11].

The noise affecting inertial sensors contains two parts: a low-frequency and a high-frequency component. Both components are combined together and affect the inertial sensor accuracy. The high-frequency component has white noise characteristics, while the low-frequency component (more commonly termed bias drift) is characterized by correlated noise. One way to deal with high-frequency noise is to de-noise the inertial sensor measurements prior to processing. In this study we can remove the effect of the short-term error of the stand-alone INS only, while the long-term error can often be modeled with sufficient accuracy as a stochastic process, and be estimated and compensated using data fusion

techniques like Kalman filter [12].

In order to enhance the final accuracy of the system especially during GPS outages, it is necessary to use an appropriate pre-filtering method to the raw IMU data. Applying efficient pre-filter successfully improves the sensors signal-to-noise ratios, removes short-term errors mixed with motion dynamics, and provides more reliable data. Conventional de-noising methods include moving average and low-pass filtering techniques. In recent years, wavelet decomposition is more often presented as an effective method to cope with the inertial sensor noise. Several other novel methods, such as neural network de-noising [13] have also been widely investigated. The wavelet enormous advantages compared with other methods of signal processing are summarized by Sifuzzaman et al. [14]. In these methods, preventing over-smoothing effects is too difficult, because there is no rigorous criterion to evaluate the cut-off frequency or the wavelet de-noising levels [15].

The wavelet transform (WT) is a powerful tool for signal and image processing. From the mid-1980s, it has been successfully used in many scientific fields such as signal processing, image compression, computer graphics, pattern recognition and de-noising of medical imaging [16]. One way to remove high frequency noise of the inertial sensor signals is to use wavelet technique prior to processing. Wavelet decomposition is a process in which a signal is successively broken down into low and high-frequency components [12,17]. Several studies have focused on evaluating the advantages of this technique, for instance, Nassar [17], Chiang et al. [10], and Abdel-Hamid et al. [18]. Skaloud [12] used wavelet decomposition technique for de-noising of INS data and achieved a significant reduction in estimated attitude errors. Bruton et al. [19] used WMRA to improve the estimation of airborne gravity disturbance values. Zhang et al. [20] also introduced a model using wavelet multi-resolution analysis and neural network to assist KF when GPS outages happen. The trained neural network can be employed to remove high-frequency noise and improve system accuracy. Noureldin et al. [21] integrated neuron-wavelet algorithm and Kalman filter to de-noising and fused the outputs of INS/GPS and provided precise positioning information for the vehicle.

In this paper, the wavelet multi-resolution analysis (WMRA) technique has been implemented experimentally to a set of tactical grade IMU (gyro

drift of 1.0–10.0 *deg/h* and accelerometer bias of 1-5 *mg*) in order to minimize the undesirable effects of sensor noise and other high-frequency disturbances. In Sect. 4, we show that the position errors obtained from de-noised INS data will be smaller than the ones obtained from the original data.

This paper is organized as follows: Section 2 describes the basic information of the Wavelet transform (WT) and the principle of wavelet multi-resolution analysis. Section 3 presents wavelet de-noising method implemented to the INS/GPS integrated navigation system. It contains the structure of INS/GPS integrated system and Kalman filter used in the integration of the system. The experimental results and the effect of de-noising INS data in INS/GPS integration with some simulated GPS outages are analyzed in section 4. Finally, the conclusion is given in section 5.

2- Wavelet de-noising technique

2- 1- Discrete wavelet transform (DWT)

Wavelet transform is able to eliminate noise and compression of signals without the original signal deterioration. The wavelet transformation of a time-domain signal is defined in terms of the projections of this signal into a family of functions that are all normalized dilations and translations of wavelet functions [22]. Wavelet techniques are based on analyzing a signal through signal windowing but with variable window sizes. The major advantage of wavelets transform relative to other signal processing techniques is a capability to analyze a localized portion of a large signal [23]. This is possible since wavelet transform applies the wide window (long time intervals) to analyze a low-frequency component of the signal and the narrow window (short time intervals) to analyze a high-frequency component of the signal [24].

The low frequency fraction of the IMU sensor data is the signal of interest (motion dynamics) and the high frequency component is usually the signal noise. In the implementation of the DWT, the wavelet coefficients of a signal are computed by passing such a signal through two complementary half-band filters, the output of the low-pass filter (LPF) is called approximation part while the output of high-pass filter (HPF) is called details part (see Fig. 1). For more details on the design of decomposition and corresponding reconstruction LPF and HPF, see [25]. A good review of statistical properties of wavelet

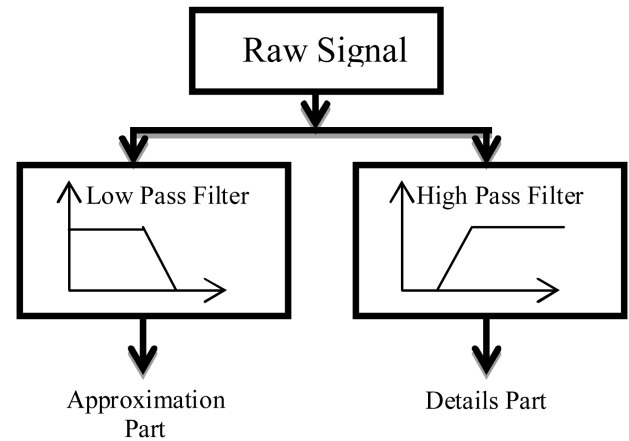


Fig. 1. Signal Decomposition by the Discrete Wavelet Transform [12]

coefficients can be found in [26] and [27].

Since we are dealing with discrete-time inertial sensor signals, the DWT is implemented. The wavelet coefficients of a discrete time sequence, $x(n)$, is given as [25,28]:

$$a_{j,k} = 2^{-j/2} \sum_n x(n) \Phi(2^{-j}n - k) \quad (1)$$

$$d_{j,k} = 2^{-j/2} \sum_n x(n) \Psi(2^{-j}n - k) \quad (2)$$

where $a_{j,k}$ and $d_{j,k}$ are the approximation coefficient and the details coefficient at the j -th resolution level, respectively, $\Phi_{j,k}(n)$ is the scale function, $\Psi_{j,k}(n)$ is the wavelet function and $2^{-j/2}\Phi(2^{-j}n-k)$, $2^{-j/2}\Psi(2^{-j}n-k)$ are the scaled and shifted versions of $\Phi_{j,k}(n)$ and $\Psi_{j,k}(n)$ respectively, based on the values of j (scaling coefficient) and k (shifting coefficient). The original signal $x(n)$ can be generated from the corresponding wavelet function using the following equation:

$$x(n) = \sum_{k=-\infty}^{\infty} a_{j,k} \phi_{j,k}(n) + \sum_{j=-\infty}^{\infty} \sum_{k=-\infty}^{\infty} d_{j,k} \Psi_{j,k}(n) \quad (3)$$

The wavelet function should be short and oscillatory; in other words, it should have zero average and decay quickly at both ends. This condition ensures that the summation in the DWT equation is finite [29,30].

2- 2- Signal de-noising using Wavelet multi-level of decomposition

The wavelet multi-resolution analysis or wavelet multiple Level of Decomposition (LOD) is a procedure in which a signal is broken down into various resolution levels [12,23]. Therefore, to obtain finer resolution frequency components

of a specific signal, the signal is broken down into many lower-resolution components by repeating the DWT decomposition procedure with successive decompositions of the obtained approximation parts (see Fig. 2). Using wavelet multi-resolution analysis, the signal can be represented by a finite sum of components at different resolutions and hence, each component can be processed adaptively depending on the application at hand [23]. Applying WMRA to the inertial signal comprises two main steps. The first involves eliminating the high-frequency sensor noise using wavelet de-noising methods. The second step then follows by specifying a proper threshold through which the motion dynamics can be separated from the short-term and/or long-term sensor errors as well as other disturbances. The approximation part includes the long term noises, the earth gravity and rotation rate frequency and dynamic of vehicle motion. The WMRA is unable to separate long-term noise and the IMU readings. Thus, it must be removed by the appropriate integration algorithm using auxiliary sensors. The details part includes the undesired high-frequency noise components of the IMU and a lot of noise disturbances such as vehicle vibration.

The WMRA algorithm is presented in four main stages to remove noise from the data:

1) Choosing an appropriate value for LOD is very important. The selection is based on the removal high-frequency noise while keeping all the useful information in the signal. LOD selection criteria for static and kinematic mode data have been further reviewed in [31]. To select an appropriate LOD for static inertial data, several decomposition levels are applied and the standard deviation (STD) value of the high frequency component can be calculated for each

obtained approximation component. The acceptable LOD will be the one after which the STD reaches its minimum value. To select an appropriate LOD for kinematic inertial data, in the beginning, a spectral analysis of the kinematic INS sensor raw data should be performed to ensure that the de-noising process does not remove any actual motion information. The vehicle motion dynamics is usually in the low-frequency portion of the spectrum. Then, by analyzing the spectrum, the frequency range of dynamic motion is detected. Therefore, the appropriate LOD can be selected to remove only the components that have frequencies higher than the detected motion frequency range.

2) Selection of the appropriate wavelet function. The wavelet transform has various types of filters such as Daubechies, Coiflet, BiorSplines and Symlets which have different coefficients. To achieve optimal performance in de-noising and minimize RMSE in navigation, one needs to choose an appropriate wavelet function.

3) Then, in order to reject the noise, a threshold is set for the obtained detail coefficients at each level. Setting a threshold can be classified into hard and soft thresholding as described by Burrus et al. [22]. The choice of the threshold value is crucial to the quality of the de-noising process. Several different methods were offered to calculate the amount of threshold by Ma et al. [32], Li and Zhao [33], Veterli et al. [34] and Misite et al. [35].

4) Reconstruct the de-noised signal using the linear combination of the details and approximation coefficients which have been obtained at each level. Then, the inverse wavelet transform is applied to this de-noised signal.

3- INS-GPS integrated navigation system using wavelet-based de-noising method

The structure of the INS/GPS integration system used in this study is shown in Fig. 3. The state variables, X_k , of the error state Kalman filter consist of position error, velocity error, attitude error, accelerometer bias, and gyro bias. The measurement vector, Y_k , of the Kalman filter is the position error between the states and the new measurement of GPS. Inertial sensor signal after the noise removal process has been used for INS.

The de-noising algorithm is implemented to the inertial sensor as follows. Spectral analysis is used to static and kinematic data of the gyros

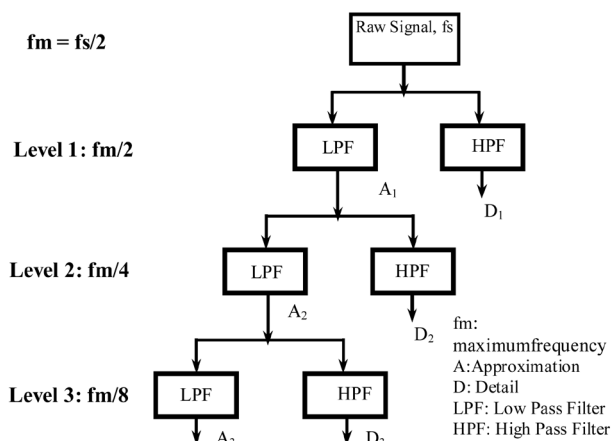


Fig. 2. Wavelet multi-resolution analysis (considering three levels of decomposition) [12]

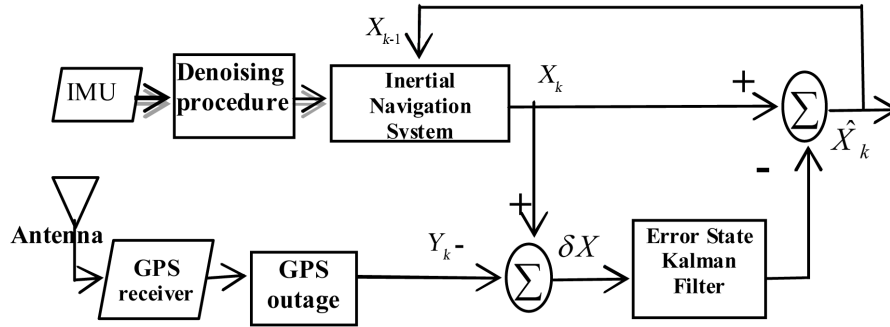


Fig. 3. IMU/GPS integrated navigation system structure

and accelerometers and the appropriate LOD of each signal is acquired. The wavelet transform is applied to calculate the coefficients and then, the inverse wavelet transform is used to reconstruct the decomposed signal. The de-noised signal is used to execute the INS/GPS integrated navigation. The process is described briefly in the flowchart shown in Fig. 4.

The following, firstly, the equations related to the position, velocity, orientation and bias in an SDINS are briefly reviewed. In the following, the system and measurement error states equations for navigation and procedure of the KF are described.

3- 1- The SDINS

The acceleration and angular rate measurement vectors of the accelerometer and gyroscope $\tilde{\mathbf{f}}^b$ and $\tilde{\boldsymbol{\omega}}_{ib}^b$ respectively, are modeled by:

$$\tilde{\mathbf{f}}^b = \mathbf{f}^b + \mathbf{b}_a + \mathbf{q}_a \tag{4}$$

$$\tilde{\boldsymbol{\omega}}_{ib}^b = \boldsymbol{\omega}_{ib}^b + \mathbf{b}_g + \mathbf{q}_g \tag{5}$$

where b and q are bias and measurement noise, respectively. The acceleration and angular rate vectors are corrected as follows:

$$\hat{\mathbf{f}}^b = \tilde{\mathbf{f}}^b - \hat{\mathbf{b}}_a \tag{6}$$

$$\hat{\boldsymbol{\omega}}_{ib}^b = \tilde{\boldsymbol{\omega}}_{ib}^b - \hat{\mathbf{b}}_g \tag{7}$$

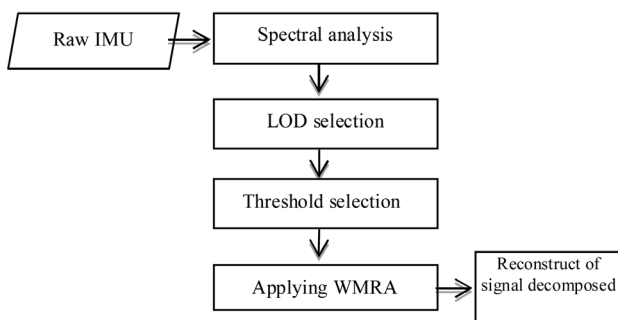


Fig. 4. Flowchart of the De-noising procedure

The accelerometer and gyro bias are modeled as random walks plus random constants, where:

$$b_a = b_{aC} + \int \boldsymbol{\omega}_{ba} dt, \boldsymbol{\omega}_{ba} \sim N(0, \sigma_{ba}^2) \tag{8}$$

$$b_g = b_{gC} + \int \boldsymbol{\omega}_{bg} dt, \boldsymbol{\omega}_{bg} \sim N(0, \sigma_{bg}^2) \tag{9}$$

where b_{aC} and b_{gC} are random constants, $\boldsymbol{\omega}_{ba}$ and $\boldsymbol{\omega}_{bg}$ are driving noise vectors assumed to be Gaussian white noise with zero mean and known variances, σ_{ba}^2 and σ_{bg}^2 , respectively.

The system state vector, x , consists of position, velocity, attitude, and bias. The vector is estimated by numerical integration of the IMU measurements and dynamic equations of the system.

$$\hat{\mathbf{x}} = [\hat{L}, \hat{l}, \hat{d}, \hat{v}_N, \hat{v}_E, \hat{v}_D, \hat{\phi}, \hat{\theta}, \hat{\psi}, \hat{b}_{ax}, \hat{b}_{ay}, \hat{b}_{az}, \hat{b}_{gx}, \hat{b}_{gy}, \hat{b}_{gz}]^T \tag{10}$$

where \hat{L} , \hat{l} and \hat{d} are latitude, longitude, depth, and \hat{v}_N , \hat{v}_E and \hat{v}_D are east velocity, north velocity, down velocity and $\hat{\phi}$, $\hat{\theta}$ and $\hat{\psi}$ are rolled angle, pitch angle, azimuth and b is the accelerometer bias and \hat{b}_g is gyro drift. The equations related to the calculation of the position, velocity, orientation and bias in an SDINS can be expressed as follows:

$$\dot{\hat{L}} = \frac{\hat{v}_N}{R_N + \hat{d}} \tag{11}$$

$$\dot{\hat{l}} = \frac{\hat{v}_E}{(R_E + \hat{d}) \tan \hat{L}} \tag{12}$$

$$\dot{\hat{d}} = \hat{v}_D \tag{13}$$

$$\dot{\hat{\mathbf{V}}}^n = \hat{\mathbf{C}}_b^n \hat{\mathbf{f}}^b - (2\hat{\boldsymbol{\omega}}_{ie}^n + \hat{\boldsymbol{\omega}}_{en}^n) \times \hat{\mathbf{V}}^n + \hat{\mathbf{g}}^n \tag{14}$$

$$\dot{\hat{\phi}} = (\hat{\omega}_y \sin \hat{\phi} + \hat{\omega}_z \cos \hat{\phi}) \tan \hat{\theta} + \hat{\omega}_x \tag{15}$$

$$\dot{\hat{\theta}} = (\hat{\omega}_y \cos \hat{\phi} - \hat{\omega}_z \sin \hat{\phi}) \tag{16}$$

$$\dot{\hat{\psi}} = (\hat{\omega}_y \sin \hat{\phi} + \hat{\omega}_z \cos \hat{\phi}) \sec \hat{\theta} \tag{17}$$

$$\dot{\hat{b}}_a = 0 \tag{18}$$

$$\dot{b}_g = 0 \tag{19}$$

where $V^n=[v_N, v_E, v_D]$ is velocity vector resolved in the navigation frame. The variables $R_N, R_E, C_b^n, \omega_{ie}^n, \omega_{en}^n$ and g^n represent the meridian radius of curvature, the transverse radius of curvature, the transformation matrix from body to navigation axes, the angular rate of the earth expressed in the navigation frame, the angular rate of the navigation frame with respect to the earth-fixed frame and the gravity vector in the navigation frame, respectively [37].

3- 2- The system equations

The error state equation is represented as a time-varying linear system:

$$\delta \dot{X}(t) = F(t)\delta X(t) + G(t)w(t), w(t) \sim N(0, Q_c) \tag{20}$$

For the inertial navigation system, the error state vector, δX , is 15×1 and consists of the position errors, velocity errors, attitude errors and the errors in the inertial sensors and is given as follow:

$$\delta X = [\delta P^n, \delta V^n, \Psi, \delta b_a, \delta b_g] \tag{21}$$

where $\delta P^n = [\delta L, \delta l, \delta d]^T$ is the position error vector of the vehicle in the navigation frame, $\delta V^n = [\delta v_N, \delta v_E, \delta v_D]^T$ is the velocity error vector resolved in the navigation frame, $\Psi = [\delta \alpha, \delta \beta, \delta \gamma]^T$ is the orientation error vector, $\delta b_a = [\delta b_{ax}, \delta b_{ay}, \delta b_{az}]$ and $\delta b_g = [\delta b_{gx}, \delta b_{gy}, \delta b_{gz}]$ are the accelerometer bias errors and the gyro drifts in the body frame, respectively.

Where, w is the process noise due to uncertainty in the control inputs and is modeled as a white-noise vector with zero mean and a power spectral density Q_c , and may be expressed as follows:

$$w = [w_a, w_g, w_{ba}, w_{bg}] \tag{22}$$

where $w_a = [w_{ax}, w_{ay}, w_{az}]$ noise components of accelerometers and $w_g = [w_{gx}, w_{gy}, w_{gz}]$ noise components of gyroscopes and $w_{ba} = [w_{bax}, w_{bay}, w_{baz}]$ and $w_{bg} = [w_{bgx}, w_{bgy}, w_{bgz}]$ are driving noise vectors assumed to be Gaussian white noise with zero mean and known variances, σ_{ba}^2 and σ_{bg}^2 , respectively. The process noise covariance matrix, Q_c , is defined as follows:

$$Q_c = \text{diag}(\sigma_a^2, \sigma_g^2, \sigma_{ba}^2, \sigma_{bg}^2) / BW_{INS} \tag{23}$$

where σ_a^2 and σ_g^2 are the accelerator and gyroscope outputs variances and $\sigma_{ba}^2, \sigma_{bg}^2$ are the variance of accelerator bias and gyroscope bias. The parameters of inertial sensors error are gained by analyzing PSD or Allan variance. BW_{INS} is the inertial sensors bandwidth.

The equations related to the errors of the position, velocity, orientation, and bias can be expressed as follows:

$$\delta \dot{P}^n = \delta V^n \tag{24}$$

$$\delta \dot{V}^n = [f^n \times] \Psi + C_b^n \delta f^b - (2\omega_{ie}^n + \omega_{en}^n) \times \delta V^n - (2\delta\omega_{ie}^n + \delta\omega_{en}^n) \times V^n - \delta g^n \tag{25}$$

$$\dot{\Psi} = -\omega_{in}^n \times \Psi + \delta\omega_{in}^n - C_b^n \delta\omega_{ib}^b \tag{26}$$

$$\delta \dot{b}_a = -\omega_{ba} \tag{27}$$

$$\delta \dot{b}_g = -\omega_{bg} \tag{28}$$

In Eq. (20), $F(t)$ is 15×15 dynamics matrix for the stand-alone INS system which propagates the errors over time and $G(t)$ is 15×12 noise distribution matrix of the stand-alone INS system. Besides, State space equations in matrix forms as follows:

$$\begin{bmatrix} \delta \dot{P} \\ \delta \dot{V} \\ \dot{\Psi} \\ \delta \dot{b}_a \\ \delta \dot{b}_g \end{bmatrix} = \begin{bmatrix} F_{11} & F_{12} & F_{13} & 0 & 0 \\ F_{21} & F_{22} & F_{23} & C_b^n & 0 \\ F_{31} & F_{32} & F_{33} & 0 & -C_b^n \\ 0 & 0 & 0 & 0 & 0 \\ 0 & 0 & 0 & 0 & 0 \end{bmatrix} \begin{bmatrix} \delta P \\ \delta V \\ \Psi \\ \delta b_a \\ \delta b_g \end{bmatrix} + \begin{bmatrix} 0 & 0 & 0 & 0 \\ C_b^n & 0 & 0 & 0 \\ 0 & -C_b^n & 0 & 0 \\ 0 & 0 & -I & 0 \\ 0 & 0 & 0 & -I \end{bmatrix} \begin{bmatrix} \omega_a \\ \omega_g \\ \omega_{ba} \\ \omega_{bg} \end{bmatrix} \tag{29}$$

The components of the dynamics matrix, F_{ij} for the SDINS system given in the appendix are derived from the (24) to (28).

3- 3- The measurement equations

The measurement equation is expressed as follows:

$$\delta Y_k = H_k \delta X_k + r_k, r_k \sim N(0, R(t)) \tag{30}$$

where H is the measurement output matrix and r represents the measurement noise which is assumed to be a zero mean, Gaussian white-noise process with time-varying covariance matrix, $R(t)$. The measurements are the linear combination of states perturbed by measurement noise. The measurement error vector, δy_k giving the difference between the navigation solution from the SINS and auxiliary sensors signal, is given by:

$$\delta Y_k = \delta Y(t_k) = \begin{bmatrix} \hat{L}_{ins}(t_k) - L_m(t_k) \\ \hat{l}_{ins}(t_k) - l_m(t_k) \\ \hat{d}_{ins}(t_k) - d_m(t_k) \end{bmatrix} \quad (31)$$

where L_m , l_m and d_m are latitude, longitude and height measured by the GPS, Respectively.

The measurement output matrix, H , and The measurement noise covariance matrix, R_k , may be expressed as follows:

$$H = \begin{bmatrix} 1 & 0 & 0 \\ 0 & 1 & 0 \\ 0 & 0 & 1 \end{bmatrix} \quad (32)$$

$$R = \text{diag}(\sigma_L^2, \sigma_l^2, \sigma_d^2) \quad (33)$$

where σ_L^2 , σ_l^2 and σ_d^2 are the variances of the GPS's measurement.

3- 4- The integration procedure

In order to formulate the Kalman filter, Eqs. (20) and (30) are required. The implementation of the Kalman filter requires a discrete-time state transition matrix, $\Phi_{k|k-1}$, for the time interval from t_{k-1} to t_k , and a discrete-time process noise covariance matrix Q_k [4].

$$\delta X_k = \Phi_{k-1} \delta X_{k-1} + \Gamma_{k-1} w_{k-1}, \quad w_k \sim N(0, Q_k) \quad (34)$$

where $\Phi_k = \exp(F_k dt)$, $Q_k = dt[A_k G Q_c G^T A_k^T + G Q_c G^T]$ and $dt = t_k - t_{k-1}$ is the sampling time of inertial sensors and is input white noise in a time interval t_{k-1} to t_k [38].

Kalman filter algorithm consists of two main stages, in the prediction procedure; the system state and its covariance are predicted to receive measured inertial data as follows:

$$\delta \hat{X}_{k-} = 0 \quad (35)$$

$$P_{k-} = \Phi_k \hat{P}_k^+ \Phi_k^T + Q_{k-1} \quad (36)$$

When one or more of auxiliary sensors are received at the time t_k , the update procedure of the KF is executed. In the event that none of the auxiliary sensors are available, the filter continues to operate without update using the prediction procedure. On receiving a new auxiliary signal Y_k , the navigation error state $\delta \hat{X}_k^+$ and its associated covariance matrix \hat{P}_k^+ at time step t_k are corrected. The update procedure of KF is given by the following equations:

$$v_k = \delta Y_k - H_k \delta \hat{X}_{k-} \quad (37)$$

$$K_k = P_{k-} H_k^T (H_k P_{k-} H_k^T + R)^{-1} \quad (38)$$

$$\delta \hat{X}_k^+ = \delta \hat{X}_{k-} + K_k v_k \quad (39)$$

$$P_k^+ = P_{k-} - K_k (H_k P_{k-} H_k^T + R) K_k^T \quad (40)$$

where K_k is the Kalman gain which updates the weight between auxiliary measurements and the predicted states. v_k is the innovation sequence. The innovation sequence is simply the difference between the actual measurements and the predicted measurements based on the predicted state vector. Note that, it is necessary for covariance matrix to be a symmetric matrix, which can be done by replacing P with $(P+P^T)/2$.

4- Experimental result

In order to evaluate the performance of the designed system, a road test was set. An instrumented car was utilized to perform the experiments as shown in Fig. 5.

The instruments used in the test include a fiber optic gyro IMU and a GPS receiver installed on the car according to Fig. 5. The IMU consists of three orthogonal MEMS accelerometer (bias of several milli-g) and three orthogonal fiber optic gyroscope (gyro drift of 1.0 deg/h). To test the effect of de-noising inertial sensor data on the system results, the positioning performance of INS/GPS integration during GPS outages is analyzed offline.

The de-noising procedure was applied to real data set collected using tactical-grade IMU. The trajectory of the test is a closed path of the Campus of Isfahan University of Technology shown in Fig. 6. It also shows the true trajectory measured by GPS for twenty minutes travelling time.

In this work, soft thresholding and threshold value obtained by Steins unbiased risk estimation method proposed by Donoho et al. [36] are used. The de-noising result shows that Daubechies 5 wavelet filter is the best filter type used to remove the high frequency noise. The appropriate LOD must be



Fig. 5. Instrumented car for experiment



Fig. 6. Road test trajectory in the Campus of Isfahan University of Technology (Google map)

selected before performing wavelet decomposition. Therefore, to select the appropriate LOD, a spectral analysis of the raw IMU data is performed. Fig. 7 shows the spectrum of kinematic and static raw data of x -axis accelerometer. The spectral analysis clearly shows that the motion dynamics is located at low frequencies less than about 5 Hz. The maximum acceptable value of LOD that can be considered is level four.

In this test, a number of 10 GPS outages were selected and the selected outage intervals are 60 seconds. Fig. 8 shows the estimated position in the horizontal (e.g. east and north) direction of the trajectory using raw and de-noised IMU signals. Root mean square of the position and velocity errors during the selected GPS outages of both raw INS/GPS navigation and de-noised INS/GPS navigation are computed and are shown in Figs. 9 and 10,

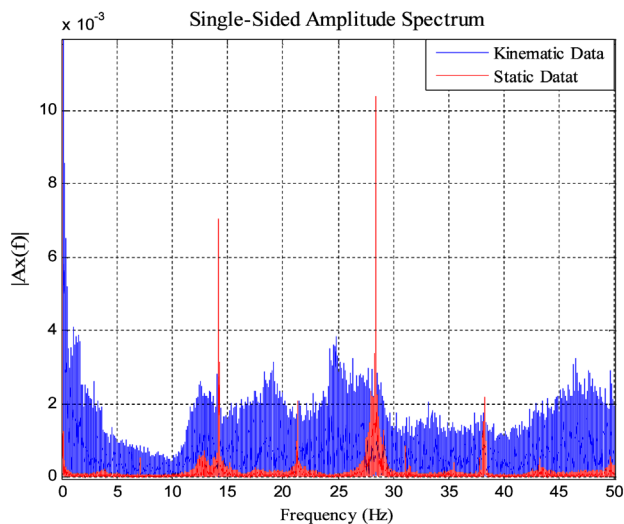


Fig. 7. The spectrum of kinematic and static raw data of x -axis accelerometer

respectively.

The position errors of INS/GPS integration during GPS outages are decreased mostly by removing the high frequency portion of the inertial sensor noises. The results show that total improvement of about 14% in root mean square of the position errors and about 12% in root mean square of the velocity errors are obtained using WMRA procedure. The average of the position errors at the end of the GPS outages obtained in a navigation system using de-noised IMU data was reduced by 18%. The results obtained from the practical test for travelled trajectories are summarized in Table 1.

It is not easy to compare the results of present work with those of others. Actually, comparisons between results require the same test conditions, such as, sensors used, traveled trajectory and a vehicle that performs the test. However, the test

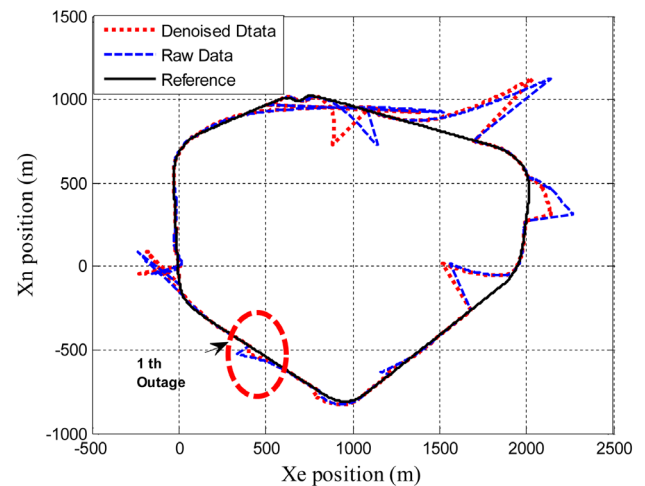


Fig. 8. Estimated positions using the raw data and de-noised data

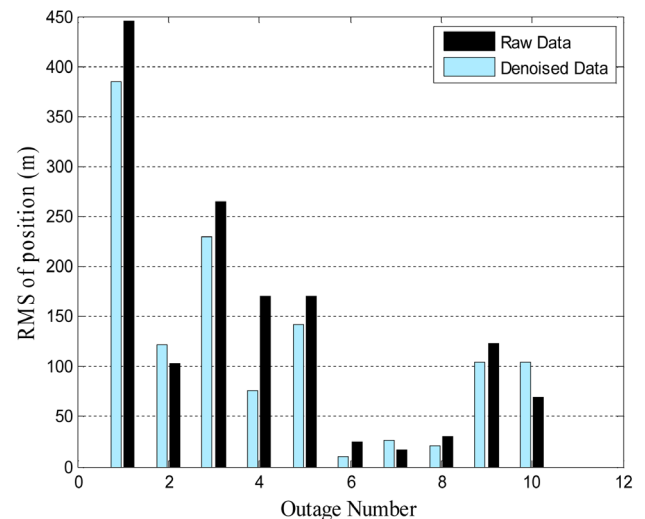


Fig. 9. RMS of position error during GPS outages

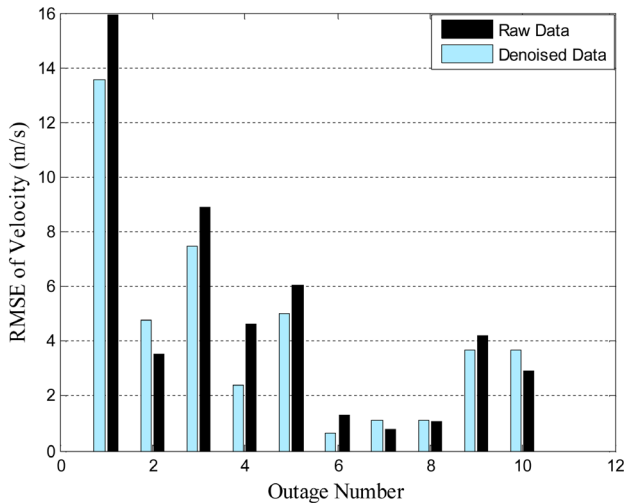


Fig. 10. RMS of velocity error during GPS outages

conditions and the results of Nassar et al. [39] are presented here. They performed two tests to evaluate the effect of de-noising inertial sensor data on the positioning performance of INS/DGPS integrated navigation system. The first test was carried out using a navigation-grade IMU in Laval, Quebec while the second test was performed using a tactical-grade IMU in Calgary, Alberta during DGPS outages. They chose a number of 10 DGPS outages, and the selected outage intervals were ranged from 70 sec. to 100 sec. and from 70 sec. to 180 sec. for the first and

Table 1. Performance comparison between raw data and denoised data in integrated navigation

Type of Data	RMSE of Position (m)		RMSE of Velocity (m/s)	
	Raw	Denoised	Raw	Denoised
Outage No. 1	445	384	15.92	13.53
Outage No. 2	103	122	3.55	4.72
Outage No. 3	264	230	8.91	7.46
Outage No. 4	170	76	4.64	2.41
Outage No. 5	169	142	6.06	5.01
Outage No. 6	24.5	9.7	1.32	0.63
Outage No. 7	16.5	25.65	0.76	1.11
Outage No. 8	30	20.44	1.07	1.12
Outage No. 9	123	104.62	4.21	3.69
Outage No. 10	69	104.18	2.92	3.66
Mean	141.78	121.96	4.93	4.33

second test, respectively. The third and fourth levels were used for the LOD of the navigation-grade and the tactical-grade IMU data, respectively. The results show that the position errors at the end of the DGPS outages were reduced by 13%–34%.

5- Conclusion

The high-frequency noise portion of inertial data causes deterioration of position accuracy of the INS/GPS integrated navigation system, especially during GPS outages. To overcome such a problem, a de-noising procedure based on WMRA technique has been used. Determining the exact value of LOD is very critical in the process of de-noising. In order to obtain an accurate LOD, spectral analysis of static and dynamic data was performed.

An experimental analysis was done using a tactical grade IMU installed on the car for a ring trajectory. The results of the road test show a 14% improvement in root mean square of the position errors during the selected GPS outages using WMRA de-noising technique. The average of the position errors at the end of the GPS outages obtained in a navigation system using de-noised IMU data was reduced by 18%.

6- Appendix

The dynamics matrices F_{ij} of the SDINS system (29) are given by:

$$F_{11} = \begin{bmatrix} 0 & 0 & -\frac{v_N}{(R_0 + d)^2} \\ \frac{v_E \tan L}{(R_0 + d) \cos L} & 0 & -\frac{v_E}{(R_0 + d)^2 \cos L} \\ 0 & 0 & 0 \end{bmatrix}$$

$$F_{12} = \begin{bmatrix} \frac{1}{(R_0 + d)} & 0 & 0 \\ 0 & \frac{1}{(R_0 + d) \cos L} & 0 \\ 0 & 0 & 1 \end{bmatrix}$$

$$F_{13} = \begin{bmatrix} 0 & 0 & 0 \\ 0 & 0 & 0 \\ 0 & 0 & 0 \end{bmatrix}$$

$$F_{21} = \begin{bmatrix} -v_E \left(2\Omega \sin L + \frac{v_E}{(R_0 + d) \cos^2 L} \right) & 0 & \frac{1}{(R_0 + d)^2} (v_E^2 \tan L - v_N v_D) \\ 2\Omega (v_N \cos L - v_D \sin L) + \frac{v_N v_E}{(R_0 + d) \cos^2 L} & 0 & -\frac{v_E}{(R_0 + d)^2} (v_N \tan L + v_D) \\ 2\Omega v_E \sin L & 0 & \frac{1}{(R_0 + d)^2} (v_N^2 + v_E^2) \end{bmatrix}$$

$$F_{22} = \begin{bmatrix} \frac{v_D}{(R_0+d)} & -2\left(\Omega \sin L + \frac{v_E}{(R_0+d)} \tan L\right) & \frac{v_N}{(R_0+d)} \\ 2\Omega \sin L + \frac{v_E}{(R_0+d)} \tan L & \frac{1}{(R_0+d)}(v_N \tan L + v_D) & 2\Omega \cos L + \frac{v_E}{(R_0+d)} \\ -\frac{2v_N}{(R_0+d)} & -2\left(\Omega \cos L + \frac{v_E}{(R_0+d)}\right) & 0 \end{bmatrix}$$

$$F_{23} = \begin{bmatrix} 0 & -f_D & f_E \\ f_D & 0 & -f_N \\ -f_E & f_N & 0 \end{bmatrix}$$

$$F_{31} = \begin{bmatrix} -\Omega \sin L & 0 & \frac{-v_E}{(R_0+d)^2} \\ 0 & 0 & \frac{v_N}{(R_0+d)^2} \\ -\Omega \cos L - \frac{v_E}{(R_0+d)\cos^2 L} & 0 & \frac{v_E}{(R_0+d)^2} \tan L \end{bmatrix}$$

$$F_{32} = \begin{bmatrix} 0 & \frac{1}{(R_0+d)} & 0 \\ \frac{-1}{(R_0+d)} & 0 & 0 \\ 0 & \frac{-\tan L}{(R_0+d)} & 0 \end{bmatrix}$$

$$F_{33} = \begin{bmatrix} 0 & -\left(\Omega \sin L + \frac{v_E}{(R_0+d)} \tan L\right) & \frac{v_N}{(R_0+d)} \\ \left(\Omega \sin L + \frac{v_E}{(R_0+d)} \tan L\right) & 0 & \Omega \cos L + \frac{v_E}{(R_0+d)} \\ -\frac{v_N}{(R_0+d)} & -\Omega \cos L - \frac{v_E}{(R_0+d)} & 0 \end{bmatrix}$$

7- References

[1] Grewal, M. S.; Weill, L. R. and Andrews, A. P.; “Global Positioning Systems, Inertial Navigation, and Integration,” *John Wiley and Sons*, 2001

[2] Kalman, R. E.; “A New Approach to Linear Filtering and Prediction Problems,” *ASME Trans. Ser. D: J. Basic Eng.*, Vol. 82, No. 1, pp. 34–45, 1960.

[3] Farrell, J. A. and Barth, M.; “The Global Positioning System and Inertial Navigation,” *McGraw-Hill Professional*, New York, 1999.

[4] Maybeck, P. S.; “Stochastic Models, Estimation and control,” *Academic Press*, New York, Vol. 1, 1979.

[5] Skog, I. and Handel, P.; “Time Synchronization Errors in Loosely Coupled GPS-Aided Inertial Navigation Systems,” *IEEE Transactions on Intelligent Transportation Systems*, Vol. 12, No. 4, pp. 1014–1023, 2011.

[6] Shabani, M.; Gholami, A. and Davari, N.; “Asynchronous Direct Kalman Filtering Approach

for Underwater Integrated Navigation System,” *Nonlinear Dyn*, Vol. 80, Nos. 1–2, pp. 71–85, 2015.

[7] Wendel, J.; Schlaile, C. and Trommer, G. F.; “Direct Kalman Filtering of GPS/INS for Aerospace Applications,” *International Symposium on Kinematic System in Geodesy, Geomatics and Navigation*, Alberta, Canada, 2001.

[8] Qi, H. and Moore, J. B.; “Direct Kalman Filtering Approach for GPS/INS Integration,” *IEEE Trans. Aerosp. Electron. Syst.*, Vol. 38, No. 2, pp. 687–693, 2002.

[9] Shabani, M.; Gholami, A.; Davari, N. and Emami, M.; “Implementation and Performance Comparison of Indirect Kalman Filtering Approaches for AUV Integrated Navigation System Using Low Cost IMU,” *ICEE*, Mashhad, Iran, pp. 1–6, 2013.

[10] Chiang, K.; Aboelmagd, N. and El-Sheimy, N.; “Constructive Neural-Networks-Based MEMS/GPS Integration Schme,” *IEEE Trans. Aerospace Electronic Syst.*, Vol. 44, No. 2, pp. 582–594, 2008.

[11] Schwarz, K. P. and Wei, M.; “Modeling INS/GPS for Attitude and Gravity Applications,” *Proceedings of the 3rd International Workshop of High Precision Navigation*, Stuttgart, Germany, Vol. 95, pp. 200–218, 1995.

[12] Škaloud, J.; “Optimizing Georeferencing of Airborne Survey Systems by INS/GPS,” *Ph.D. Thesis*, Department of Geomatics Engineering, University of Calgary, Calgary, Alberta, Canada, UCGE Report No. 20126, 1999.

[13] El-Rabbany, A. and El-Diasty, M.; “An Efficient Neural-Network Model for De-noising of MEMS-based Inertial Data,” *The Journal of Navigation*, Vol. 57, pp. 407–415, 2004.

[14] Sifuzzaman, M.; Islam, M. R. and Ali, M. Z.; “Application of Wavelet Transform and its Advantages Compared to Fourier Transform,” *Journal of Physical Sciences*, Vol. 13, pp. 121–134, 2009.

[15] Grejner-Brzezinska, D.; Torh, C. and Yi, Y.; “On Improving Navigation Accuracy of GPS/INS Systems,” *Photogrammetric Engineering and Remote Sensing*, Vol. 71, No. 4, pp. 377–389, 2005.

[16] Daubechies, I.; “Orthonormal Basis of Compactly Supported Wavelets,” *Comm. Pure Applied Math.*, Vol. 41, No. 7, pp. 909–996, 1988.

[17] Nassar, S.; “Improving the Inertial Navigation

- System (INS) Error Model for INS and INS/DGPS Applications,” *Ph.D. Thesis*, Department of Geomatics Engineering, University of Calgary, Canada, UCGE Report No. 20183, 2003.
- [18] Abdel-Hamid, W.; Osman, A.; Noureldin, A. and El-Sheimy, N.; “Improving the Performance of MEMS-based Inertial Sensors by Removing Short-Term Errors Utilizing Wavelet Multi-Resolution Analysis,” in *Proceedings of ION NTM*, San Diego CA, U.S. Institute of Navigation, pp. 260–266, 2004.
- [19] Bruton, A.; Schwarz, K. P. and Škaloud, J.; “The Use of Wavelets for the Analysis and De-noising of Kinematic Geodetic Measurements,” *Proceedings of the IAG Symposia No. 121*, Geodesy Beyond, The Challenges of the First Decade, Birmingham, UK, pp. 227–232, 2000.
- [20] Zhang, T. and Xu, X. S.; “A New Method of Seamless Land Navigation for GPS/ INS Integrated System,” *Measurement*, Vol. 45, No. 4, pp. 691–701, 2012.
- [21] Noureldin, A.; Osman, A. and El-Sheimy, N.; “A Neuro-Wavelet Method for Multi-Sensor System Integration for Vehicular Navigation,” *Meas. Sci. Technol.*, Vol. 15, No. 2, pp. 404–412, 2004.
- [22] Burrus, C. S.; Gopinath, R. and Guo, H.; “Introduction to Wavelet and Wavelet Transforms a Primer,” *Prentice Hall*, 1998.
- [23] Goswami, A. and Chan, K.; “Fundamentals of Wavelets: Theory, Algorithms and Applications,” *Wiley*, p. 359, 1999.
- [24] Ogden, R. T.; “Essential Wavelets for Statistical Applications and Data Analysis,” *Birkhäuser Boston*, 1997.
- [25] Strang, G. and Nguyen, T.; “Wavelets and Filter Banks,” *Wellesley-Cambridge Press*, 1997.
- [26] Buccigrossi, R. W. and Simoncelli, E. P.; “Image Compression via Joint Statistical Characterization in the Wavelet Domain,” *IEEE Image Process.*, Vol. 8, No 12, pp. 1688–1701, 1999.
- [27] Romberg, J. K.; Choi, H. and Baraniuk, R. G.; “Bayesian Tree-Structured Image Modeling Using Wavelet-Domain Hidden Markov Models,” *IEEE Image Process.*, Vol. 10, No. 7, pp. 1056–1068, 2001.
- [28] Mallat, S. G.; “A Theory for Multiresolution Signal Decomposition: The Wavelet Representation,” *IEEE Trans Pattern Analysis and Machine Intelligence*, Vol. 11, No. 7, pp. 674–693, 1989.
- [29] Alnuaimy, A. N. H.; Ismail, M.; Ali, M. A. M. and Jumari, K.; “TCM and Wavelet De-noising Over an Improved Algorithm for Channel Estimations of OFDM System Based Pilot Signal,” *J. Applied Sci.*, Vol. 9, pp. 3371–3377, 2009.
- [30] Putra, T. E.; Abdullah, S.; Nuawi, M. Z. and Nopiah, Z. M.; “Wavelet Coefficient Extraction Algorithm for Extracting Fatigue Features in Variable Amplitude Fatigue Loading,” *J. Applied Sci.*, Vol. 10, No. 4, pp. 277–283, 2010.
- [31] Misiti, M.; Misiti, Y.; Oppenheim, G. and Poggi, J. M.; “Wavelet Toolbox for the Use with Matlab,” *The Mathworks Inc.*, MA, USA, 2000.
- [32] Ma, X.; Zhou, C. and Kemp, I. J.; “Automated Wavelet Selection and Thresholding for PD Detection,” *IEEE Electrical Insulation Magazine*, Vol. 18, pp. 37–45, 2002.
- [33] Li, W. and Zhao, J.; “Wavelet Based De-noising Method to Online Measurement of Partial Discharge,” *Proceedings of Asia-Pacific Power and Energy Engineering Conference*, Wuhan, China, pp. 1–3, 2009.
- [34] Vetterli, M.; Chang, S. G. and Yu, B.; “Spatially Adaptive Wavelet Thresholding with Context Modeling for Image De-noising,” *IEEE Trans. Image Process.*, Vol. 9, No. 9, pp. 1522–1531, 2000.
- [35] Misite, M.; Misite, Y.; Oppenheim, G. and Poggi, J. M.; “Wavelet Toolbox: Computation, Visualization and Programming: Version 2,” *Mathworks Inc.*, California, 2002.
- [36] Donoho, D.; Iain, L. and Johnstone, M.; “Adapting to Unknown Smoothness via Wavelet Shrinkage,” *Journal of the American Statistical Association*, Vol. 90, No. 432, pp. 1200–1244, 1995.
- [37] Titterton, D. H. and Weston, J. L.; “Strapdown Inertial Navigation Technology,” *Peter Peregrinus*, UK, 1997.
- [38] Brown, R. G. and Hwang, P. Y. C.; “Introduction to Random Signals and Applied Kalman Filtering: With MATLAB Exercises and Solutions,” *Wiley*, New York, Vol. 1, 1997.
- [39] Nassar, S. and El-Sheimy, N.; “Wavelet Analysis for Improving INS and INS/DGPS Navigation Accuracy,” *The Journal of Navigation*, Vol. 58, No. 1, pp. 119–134, 2005.